



Published in final edited form as:

*Proteomics Clin Appl.* 2014 April ; 8(0): 130–142. doi:10.1002/prca.201300031.

## Aberrant Glycosylation in the Human Trabecular Meshwork:

### Aberrant Glycosylation in the Trabecular Meshwork

Adam E. Sienkiewicz<sup>1</sup>, Brandon N. Rosenberg<sup>1</sup>, Genea Edwards<sup>1,2</sup>, Teresia A. Carreon<sup>1,2</sup>, and Sanjoy K. Bhattacharya<sup>1,2,3,\*</sup>

<sup>1</sup>Bascom Palmer Eye Institute, University of Miami, Miami, FL, 33136

<sup>2</sup>Department of Biochemistry and Molecular Biology, University of Miami, Miami, FL, 33136

<sup>3</sup>Neuroscience Program, University of Miami, Miami, FL, 33136

### Abstract

**Purpose**—To determine the difference in protein glycosylation and glycosylation enzyme levels between glaucomatous and control trabecular meshwork (TM).

**Experimental design**—Glaucomatous and normal donor (n=12 each) TM tissues, Lectin-fluorescence, fluorophore assisted carbohydrate analyses, and quantitative mass spectrometry were used to determine the glycosylation levels. Primary TM cells and glycosylation inhibitors were used to determine their effect on cell shape and motility.

**Results**—In contrast to elevated levels of glycoproteins determined by lectin-fluorescence, simultaneous hyper and hypo-glycosylation in glaucomatous trabecular meshwork was revealed by fluorophore assisted carbohydrate analyses. Analyses of enzymes showed elevation of Beta-glycosidase 1 and decrease in Galactosyltransferase family 6 domain containing protein 1 in the glaucomatous trabecular meshwork. Quantitative mass spectrometry identified select protein level changes between glaucomatous and normal trabecular meshwork. Primary trabecular meshwork cells were treated with inhibitors to elicit hypo-glycosylation, which affected cell shape, motility, and fluorescent tracer transport across a layer of trabecular meshwork cells.

**Conclusions and clinical relevance**—Global protein glycosylation is aberrant in glaucomatous trabecular meshwork compared to controls. The results presented here suggest that the alteration in global TM protein glycosylation encompassing cellular and extracellular matrix proteins contributes to glaucoma pathology likely mediated through changes in properties of TM cells.

### Keywords

Trabecular meshwork; glycosylation; carbohydrate electrophoresis; glaucoma

---

\*Corresponding author: Bascom Palmer Eye Institute (McKnight Bldg.), 1638 NW 10th Avenue, Suite 706A, University of Miami, Miami, FL 33136, Tel: +1-305-482-4103 (Office), Tel: +1-305-482-4109 (Lab), Fax: +1-305-326-6547.

## 1 Introduction

The functional states of a multicellular organism are governed by a constant dynamic interaction between expression of intrinsic genetic information and environmental factors. Many of life's secrets reside at the level of modulation of the cellular signals to bring functional changes in response to altered environments. Posttranslational modifications (PTMs) are a rapid and energy cost effective means for cells to alter the information on protein structures and thereby the function in response to changing environments [1]. Their Importance in aging and in disease states are now being increasingly realized [2, 3]. Addition of sugar/glycosyl moieties on proteins is termed as glycosylation. Target proteins can exist as hypo and hyper-glycosylated at a given state of the cell compared to another state (for instance, normal to pathological). Glycosylation on two different target proteins may potentially bring two functionally opposite responses, for example, activation and deactivation.

The glaucomas are a family of progressive irreversible blinding optic neuropathies affecting over 60 million people worldwide [4]. Primary open angle glaucomas (POAGs), which usually account for a large majority, are late onset diseases. Angle closure glaucomas (ACGs) are also part of the cohort but unlike POAG they are anatomically explicable and are better intervened by opening the blocked angle by surgical means. Current medications or intervention strategies halt glaucoma progression and delay the disease process (especially POAG) but do not offer a cure [4, 5]. Glaucoma presents a large health burden with regard to quality of life and productivity. Elevated intraocular pressure (IOP) has been shown to be a major risk factor for the development and progression of glaucomatous optic nerve damage. Reduction in IOP (by pharmacological or surgical means) is the only proven neuro-protectant in delaying glaucoma progression [5]. Elevated IOP occurs as a result of reduced aqueous outflow and increased resistance at the level of the trabecular meshwork (TM), a very small region in the anterior chamber angle between the iris and cornea that serves as a filter for aqueous humor outflow [6]. Increased outflow resistance at the level of the TM presumably occurs due to changes in the cytoskeleton and the TM extracellular matrix (ECM). Due to passage of aqueous flow through this region, TM cells are expected to be responsive to mechanotransduction in response to changing shear stress. The surface proteoglycan layer (glycocalyx) acts as a sensor of fluid shear stress in endothelial and other types of cells, transmitting mechanosensation initiating responsive actions in the actin network of the cytoskeleton [7, 8].

The changes in glycoproteins and proteoglycans in the TM tissue have been the subject of prior studies [9–12]. These studies have encompassed analyses for expression of mRNA [9, 10] and proteins [13] but not the actual glycosylation changes on proteins. Poor correlation between mRNA and protein levels has been shown in previous investigations [14]. Analyses of glycosylation or any other PTMs need to be performed independent of analyses of proteins and mRNAs. Analyses of TM proteins as well as their contributing enzymes have yet to be done. This study aims to determine glycosylation changes between normal and glaucomatous TM. Furthermore, we aimed to capture the alteration of cellular properties in response to glycosylation changes induced with enzyme inhibitors in vitro.

## 2 Materials and methods

### 2.1 Tissue procurement and histochemical Lectin-binding studies

Glaucomatous and normal tissues were procured from National Disease Research Interchange (NDRI), Philadelphia, PA and from Florida Lions Eye Bank, Miami, FL respectively. All eyes used for this study were enucleated within 24 h of death, from donors who were not subjected to laser treatment (LT; Supplemental Table S1). Histochemical studies have utilized 17 biotinylated lectins (EY Laboratories Inc, San Mateo, CA) at a working concentration of 9 µg/ml, 3, 3'-diaminobenzidine (DAB), horseradish peroxidase (HRP) and published protocols [15, 16], or Alexa-594 conjugated streptavidin (Invitrogen Inc., Carlsbad, CA) for the immunofluorescent detection of bound lectins (Supplemental Table S2). Images were taken on a Leica TSP5 confocal microscope (Leica Corporation, Manheim, Germany) and quantified using Image J software (Rasband W.S, U.S. NIH, Bethesda, MD). All experiments and procedures were reviewed and approved by the University of Miami's institutional review boards and are in accordance with the declaration of Helsinki. All histochemical data presented here are representative of several analyses (n= 12 each glaucoma and controls) performed during this study.

### 2.2 Fluorophore-Assisted Carbohydrate Electrophoresis (FACE)

FACE analyses of protein extracts prepared from 20 mg of normal and glaucomatous TM were performed following published protocols [17, 18]. Briefly, proteins were digested with 10 µl of Bovine testicular Hyaluronidase (0.5 U) and Chondroitinase ABC (10 U), divided into two equal aliquots (control and mercuric acetate treatment), and electrophoresed with standards in a Dermato-or-Hyaluro-Disaccharide Kit (Seikagaku Corporation, Japan). All samples were derivatized using 2-Aminoacridone prior to electrophoresis on a Monosaccharide polyacrylamide gel (Glyko/Prozyme, San Leandro, CA). Following electrophoresis, the gel was illuminated under UV light (365 nm) and imaged using ChemiDoc XRS+ System (Bio-Rad Labs).

### 2.3 Quantitative Proteomics

We utilized 12 glaucomatous and 12 normal samples for 8 plex ITRAQ labeling using a kit (cat# 4390811, Applied Biosystems, Carlsbad, CA) containing 113–119 and 121 isotopic tags following procedures routinely used in our laboratory [19]. The samples were analyzed on an ABI 4800 MALDI TOF-TOF machine (Applied Biosystems, Carlsbad, CA). Quantitative proteomics were separately performed for both the TM protein extracts as well as for lectin immunoprecipitation products. Quantification of lectin immunoprecipitation products was done as follows: briefly, protein extracts were prepared from glaucomatous and normal donor TM using 100µl of the buffer 125 mM Tris-HCl (pH 7.0), 100 mM NaCl, 0.1% Triton X-100, and 0.1% Genapol C-100 per 25mg of tissue. The homogenized suspension was centrifuged at 10,000 rpm and precipitated using 10µl of a 9µg/µl working concentration of a biotinylated lectin, (for example, *Caragana arborescens* lectins; Supplemental Table S5). The precipitate was recovered with 25 µl of 4µg/µl streptavidin coupled magnetic beads (cat# S1420S, New England Biolabs, Ipswich, MA). The eluent was subjected to acetone precipitation using a 4: 1 ratio of acetone to eluent (v/v) following standard procedures. The IP products were subjected to 8-plex iTRAQ labeling [19].

## 2.4 Mass Spectrometric analyses

To identify the proteins and perform quantification, protein bands separated on 10% SDS-PAGE were excised, the gel slices were destained with 50% acetonitrile/water and were suspended in 0.5 M triethylammoniumbicarbonate (TEAB; number 17902 Sigma Chemical Co., St. Louis, MO) pH 8.5 and reduced with 10 mM Tris-(2-carboxyethyl) phosphine (TCEP; Sigma Chemical Co., St. Louis). The proteins were subsequently alkylated in the dark using 55 mM solution of iodoacetamide (Catalog No-RPN6302V; GE Healthcare Inc., Buckinghamshire, England) and in-gel digested with sequencing grade-modified trypsin (catalog number V5113, Promega Corporation, Madison, WI 0.1 µg/15 µl in 15 mM N-ethylmorpholin) overnight at 37°C. The peptides were extracted twice with 50 µl 0.1% Trifluoroacetic acid/60% acetonitrile and finally with 30 µl of acetonitrile and dried in a SpeedVac. The extracted peptides were incubated with 8 plex iTRAQ reagents in 0.5 M TEAB containing 60% v/v isopropanol. Peptides derived from protein bands of glaucomatous TM tissue were subjected to incubation with reagents 113, 114, 115 and 116 (4381557; 4381557; 4381557; 4381560; ABI, Foster City, CA) whereas peptides derived from control TM protein bands were incubated with reagents 117, 118, 119 and 121 (4381561; 4381562; 4381563; 4381564). The incubation mixtures were dried in a SpeedVac, mixed together and loaded onto a slurry of 500 µL of cation exchange buffer in 12 mM Ammonium Formate in 25% acetonitrile at pH 2.5–3.0, and subjected to chromatographic separation.

**2D-LC separations**—SCX separations of peptides were performed on a passivated Waters 600E HPLC system, using a 4.6 × 250 mm Poly sulfoethyl aspartamide column (PolyLC, Columbia, MD) at a flow rate of 1 ml/min. Buffer A contained 10 mM ammonium formate, pH 2.7, in 20% acetonitrile/80% water. Buffer B contained 666 mM ammonium formate, pH 2.7, in 20% acetonitrile/80% water. The gradient was Buffer A at 100% (0–22 minutes following sample injection), 0% to 40% Buffer B (16–48 min), 40% to 100% Buffer B (48–49 min), then isocratic 100% Buffer B (49–56 min), then at 56 min switched back to 100% Buffer A to re-equilibrate for the next injection. The first 26 ml of eluant (containing all flow-through fractions) was combined into one fraction, then 14 additional 2 ml fractions were collected. All 15 of these SCX fractions were dried down completely to reduce volume and to remove the volatile ammonium formate salts, then resuspended in 9 µl of 2% (v/v) acetonitrile, 0.1% (v/v) trifluoroacetic acid and filtered prior to reverse phase C18 nanoflow-LC separation. For second dimension separation by reverse phase nanoflow LC, each SCX fraction was autoinjected onto a Chromolith CapRod column (150 × 0.1 mm, Merck) using a 5 µl injector loop on a Tempo LC MALDI Spotting system (ABI-MDS/Sciex). Buffer C was 2% acetonitrile, 0.1% trifluoroacetic acid, and Buffer D was 98% acetonitrile, 0.1% trifluoroacetic acid. The elution gradient was 95% Buffer C/5% Buffer D (2 µl per minute flow rate from 0–3 min, then 2.5 µl per minute from 3–8.1 min), 5% Buffer D to 38% Buffer D (8.1–40 min), 38% Buffer D to 80% Buffer D (41–44 min), 80% Buffer D to 5% Buffer D (44–49 min) (initial conditions). Flow rate was 2.5 µl/min during the gradient, and an equal flow of MALDI matrix solution was added post-column (7 mg/ml recrystallized CHCA (α-cyano-hydroxycinnamic acid), 2 mg/ml ammonium phosphate, 0.1% trifluoroacetic acid, 80% acetonitrile). The combined eluant was automatically spotted

onto a stainless steel MALDI target plate every 6 seconds (0.6  $\mu$ l per spot), for a total of 370 spots per original SCX fraction.

After drying the sample spot mentioned above, thirteen calibrant spots (ABI 4700 Mix) are added to each plate manually. MALDI target plates (15 per experiment) were analyzed in a data-dependent manner on an ABI 4800 MALDI TOF-TOF. As each plate is entered into the instrument, a plate calibration/MS Default calibration update is performed, and then the MS/MS default calibration is updated. MS spectra were taken from 5500 MALDI Spots, averaging 500 laser shots per spot at Laser Power 3100. A total of 3249 MS/MS spectra was taken with up to 2500 laser shots per spectrum at Laser Power 3600, with CID gas Air at 1.2 to  $1.3 \times 10^{-6}$  Torr. After the MS and MS/MS spectra from all 15 plates in a sample set have been acquired, protein identification and quantitation was performed using the Paragon algorithm as implemented in Protein Pilot 3.0 software (from ABI/MDS-Sciex) and Matrix Sciences Mascot algorithm version 2.1. ProteinPilot Software was utilized for searches with following search parameters: Cys Alkylation – Iodoacetamide; ID Focus – Biological Modifications; Search Effort – Thorough. For trypsin digestion 0 missed cleavages were specified. The variable PTMs, which were searched, were: Deamidation, oxidation, Carbamidomethylation and acetylation. The Jan 1st 2010 Human NCBI database Sequences containing 512785 Protein Sequences, plus 156 common lab contaminants. For estimation of “False Discovery Rate” (FDR), a simultaneous search was performed on a concatenated Decoy database, which is the exact reverse of each protein sequence in the database plus 156 common human and lab contaminants. Total Protein Sequences searched in Database plus contaminants plus concatenated Reverse Decoy Database: 1025652. The protein identifications at 95% confidence level were retained. The preset “Thorough” (iTRAQ or Identification) search settings were used where identifications must have a ProteinPilot Unused Score > 1.3 (>95% Confidence interval). In addition, the only protein IDs accepted MUST have a local “FDR” estimation of no higher than 5%, as calculated from the slope of the accumulated Decoy database hits by the PSPEP (Proteomics System Performance Evaluation Pipeline) program[20]. This local FDR estimate is much more stringent than  $p < 0.05$  or 95% confidence scores in Mascot, Sequest, ProteinPilot, or the aggregate False Discovery Rate estimations (2 X number of Decoy database IDs/Total IDs at any chosen threshold score) commonly used in the literature, and combined with the ProGroup algorithm included in ProteinPilot gives a very conservative as well as fully MIAPE-compliant list of proteins identified (i.e., Mascot and other lists of “Proteins ID’d at  $p < 0.05$ ” will produce more numerous “significant” IDs from the same data, but those larger lists are highly likely to contain many more False Positive IDs).

## 2.5 Bioinformatics, analyses of enzymes and glycosylation

A list of deglycosylases and glycosyltransferases was compiled after extensive search using literature, BRENDA, FRENDA, AMENDA and Ensembl databases. Next, a boolean search was carried out using keywords “trabecular meshwork” and “eye” in Gene Expression Omnibus (GEO) and in UniGene databases (National Center for Biotechnology Information, Bethesda, MD). The presence of mRNA for specific deglycosylases and glycosyltransferases (Table S3) identified by microarray analyses in the TM was verified using appropriate primer pairs along with PCR analysis using standard protocols. For

enzymes whose mRNA was confirmed to be present in the TM (Supplemental Table S3), further ELISA and dot blot analyses were performed. Commercially available primary antibodies for GLT8D1, GLT8D2, GLT6D1 and UGT8 (cat# ab83758, ab105655, ab80904, ab84288, Abcam Inc., Cambridge, MA), and GLA, NAGA, GLB1 ( $\beta$ -galactosidase1), FUS2, GALNS and FUCA1 (cat# ab70520, ab102668, ab616, ab93660, ab76400, ab69957, Abcam Inc.) were used for ELISA and dot blot analyses following published procedures [19]. For dot blot analyses, proteins were spotted as 0.5mm diameter spots. No protein extracts or saturated amount of protein extracts [ $>50\mu\text{g}$  on 0.5mm spot using vacuum concentrated (10mg/ml) protein extract] were used to set 0 and 100 percent level respectively for dot blot. The protein extract (1  $\mu\text{g}$ ) of a single TM extract was used to determine GAPDH and enzymatic immunoreactivity for each individual enzyme by dot blot. The densitometric determination of individual enzymatic immunoreactivity for each enzyme was normalized to GAPDH immunoreactivity and the mean result for 12 glaucomatous and 12 normal samples were determined. This normalized immunoreactivity is referred to as relative immunoreactivity. A similar analysis was carried out by ELISA for all 12 glaucomatous and normal samples determining immunoreactivity of each individual enzyme. Normalizing to GAPDH immunoreactivity (referred to as relative immunoreactivity) for 1  $\mu\text{g}$  protein extract for each TM sample and mean values for each group was determined also. For ELISA no protein and 100 $\mu\text{g}$  of GAPDH or saturating level of protein extract ( $\sim 0.9$  absorbance) was used to set 0 and 100 percent level. The dot blot densitometric quantification was performed using Image J software normalized using GAPDH immunoreactivity. The total TM proteins (10  $\mu\text{g}$ ) subjected to partial digestion for 0.5 and 1 h using 20 units of PNGase F (cat# P0704S, New England BioLabs, Ipswich, MA) were subjected to Western analysis (digests and controls) using antibodies against specific proteins. Total glycosylated proteins were also detected using Gelcode Glycoprotein kit (cat# 24562; Pierce Biotechnology, Rockford, IL) and also a Pro-Q Emerald 300 glycoprotein kit (cat# P21857; Invitrogen) following previously described procedures [21].

## 2.6 Glycosyltransferase/de-glycosylase Activity Assay Methods

In the first protocol, the wells of a 96 well plate were coated with 10  $\mu\text{l}$  (0.5  $\mu\text{g}$ ) lactotriaosylceramide (Lc3Cer) methanol solution and 50  $\mu\text{l}$  of 0.08% polyisobutylmethacrylate in a solvent mixture of chloroform/hexane/chloroform (1:5.25:25 v/v/v). Solvent was evaporated using a hair dryer and 50  $\mu\text{l}$  of 1% Bovine Serum Albumin (BSA) in 1X Phosphate Buffered Saline (PBS) was added for blocking for 2 h. Wells were washed with 1X PBS and pH was adjusted with 25  $\mu\text{l}$  of 50 mM cacodylate buffer (pH 6.8 if UDP-galactose; 8.5 when UDP-glucose is used as acceptor) containing 0.005% Triton CF-54, 0.2 M KCl, 20 mM  $\text{MnCl}_2$ , and 1.56 mM UDP-galactose and 10  $\mu\text{g}$  of protein test samples or bovine milk galactosyltransferase (25  $\mu\text{l}$ ; 250/ $\mu\text{U}$ ) as control and incubated at 37°C for 2 h. Wells were washed with 1X PBS and incubated with 50  $\mu\text{l}$  carbohydrate sequence specific monoclonal antibody 1 $\mu\text{g}/\text{ml}$ ; in PBS for 2 h at 25°C. After washing with 1X PBS, 50  $\mu\text{l}$  of alkaline phosphatase conjugated secondary antibody and 100  $\mu\text{l}$  of phosphatase substrate was added then incubated for 30 minutes followed by several washes with 1X PBS and absorbance measurement at 405 nm. A modified protocol used bovine milk galactosyltransferase, *Clostridium perfringens* sialidase with NeuAc $\alpha$ 2-3nLc4ceramide (1  $\mu\text{g}$ ) as substrate and monoclonal antibody H-11 for recognizing Gal $\beta$ 1-4GlcNAc $\beta$  as

product was used. In the second protocol that measured glucosaminidase activities, test TM protein solutions or purified N-acetyl- $\beta$ -Glucosaminidase enzyme was incubated at 37° for 30 min with 0.264mM methyl-umbelliferyl N-acetyl- $\beta$ -glucosaminide (prepared from 4-methylumbelliferone and acetochloroglucosamine) in 0.05 M sodium citrate buffer pH 5.0. The enzymatic reaction was stopped and methylumbelliferone was converted into the anionic form by addition of 0.2 M sodium glycinate buffer pH 10.65 (3 ml) at the end of incubation. The activity was estimated by measuring absorbance at 365 nm.

## 2.7 TM cell culture and inhibitor and tracer transport studies

Primary human TM cells were cultured from cadaveric corneo-scleral sections using protocols routinely used in our laboratory [13]. Time-lapse microscopy was performed using cells grown on glass bottom chamber slides (cat# 154534, Lab-Tek, Thermo Fisher Scientific Inc., Rochester, NY). Pre-incubated cells in serum-free media (DMEM, Mediatech) were further incubated for 4 h with the three inhibitors: SS: 150 $\mu$ M, PhQ: 75  $\mu$ M, MeQ: 50  $\mu$ M (1-3X of the IC50 for sulfotransferase or sialyltransferase) prior to time lapse microscopy using the Zeiss AxioVert 200M microscope with cell culture setup (Carl Zeiss Inc) inside a temperature controlled chamber at 37°C in 5% CO<sub>2</sub> atmosphere.

To achieve inhibition of glycosyltransferases and deglycosylases in vitro we employed synthetic inhibitors N-(8-quinolinylsulfonyl)-phenylalanine (PhQ; cat# OSSL\_288713, Princeton BioMolecular Research Inc., Monmouth Junction, NJ) and 4-(methylsulfanyl)-2-(quinolin-2-ylformamido)-butanoic acid (MeQ; cat# EN300-59129, Ryan Scientific, Isle of Palms, SC) (specific for GlcNAc-6-O-Sulfotransferase family) and a natural compound Soyasaponin I (SS) [(3 $\beta$ ,4 $\beta$ ,22 $\beta$ )-22,23-Dihydroxyolean-12-en-3-yl O-6-deoxy- $\alpha$ -L-mannopyranosyl-(1-2)-O- $\beta$ -D-galactopyranosyl-(1-2)- $\beta$ -D-glucopyranosiduronic acid] (SS; cat# ABS-00019336-005, Chromadex, Irvine, CA) -an inhibitor of ST3 beta-galactoside-alpha-2,3-sialyltransferase 1 (ST3GAL1).

An 8  $\mu$ m pore-size 1 cm diameter polycarbonate membrane well insert (cat# 140644, NalgeNunc International, Rochester, NY) was used to measure fluorescein sodium salt (cat# 46960, Sigma-Aldrich) flow through a multilayer (~5) matrix of primary TM cells colonized specifically for this experiment by repeating cellular suspension depositions daily. Briefly, the first layer of confluent cells (~0.5 $\times$ 10<sup>6</sup> initial cell load) was made on the membrane using routine culture techniques and incubated for 16–24 h. The second cell suspension was (~1 $\times$ 10<sup>6</sup> initial cell load) carefully distributed on the top of the first layer and allowed to assemble as a cohesive bilayer during an additional 16–24 h incubation time. The latter step was repeated four times. A second set of experiments was performed using a layer of collagen matrix (rat tail collagen; catalog #354249; BD Biosciences, San Jose, CA) formed on the membrane to facilitate cell adherence prior to the introduction of the first cell monolayer. The cells were similarly allowed to form a confluent monolayer over a period of 16–24 h. This process was repeated to ultimately achieve a confluent penta-layer of cells. Cells treated with inhibitors were pre-incubated in serum free media (Mediatech) and inhibitors for 4 h as described above. Following inhibitor treatment, the layered cell matrix was washed twice with warm 1X PBS (Mediatech). A 10 $\mu$ l volume of sodium fluorescein dye (1:100 dilution of 1 mg/ml) was introduced into the inner well of the matrix bearing

membrane insert suspended in a 500 $\mu$ l volume of 1X (PBS). The sampling was initiated and continued at 2 min intervals by aspirating from the outer well of the insert; the fluorescence of the samples were measured at 485 and 525 nm excitation and emission using a spectrofluorometer (Lumistar, BMG Labtech, Offenburg, Germany). A Trypan blue exclusion assay of primary TM cells was performed for determination of cell viability following previously published procedures[22].

## 2.8 Data and analyses

ELISA, dot blot and tracer transport results are expressed as mean $\pm$  standard deviation (SD). ELISA, dot blot and tracer transport results were compared between control and glaucoma donors by the two-tailed two sample t-test. Ratios of glaucoma to normal proteins and glycosylation levels were compared to 1.0 by the two-tailed paired or unpaired t-test.

## 3 Results

### 3.1 Simultaneous hypo and hyper protein glycosylation in glaucomatous TM

Fluorescent histochemical detection of glaucomatous and normal human TM specimens (Supplemental Table S1) with biotin-bound lectins suggested presence of elevated glycoproteins or proteoglycans in the glaucomatous TM (Figure 1A and Supplemental Table S2). These results are consistent with a previous study employing DAB [15], to detect lectin binding in the human TM. Compared to lectin-fluorescence analyses (Figure 1A), DAB lectin analyses are relatively subjective (Supplemental Figure S1A). The 7 out of 17 lectins used in our analyses were common with previous studies and showed general agreement with previous findings with only a few differences (Supplemental Table S2). We next analyzed glycosylation of human TM tissue proteins using enzymatic digestion of protein-bound sugars and FACE [17, 18] that revealed (Figure 1B) simultaneous presence of hypo and hyper- protein glycosylation in glaucomatous TM compared to the controls. This is in contrast to the lectin-fluorescence analyses (Figure 1A). The observed difference between lectin-bound fluorescence (Figure 1A) and FACE (Figure 1B) could be reconciled in the following way, that hyper-glycosylated moieties in the glaucomatous TM are probably more exposed epitopes compared to that in the normal controls (Figure 1B), while the hyper-glycosylated moieties in the controls, as revealed by FACE (Figure 1B), are either buried or not recognized by lectins (Figure 1A). The FACE analyses (Figure 1B) showed simultaneous occurrence of both hypo and hyper-glycosylation in the glaucomatous TM. To ensure that equal amount of protein extract was utilized for these analyses between control and glaucoma groups, an identical aliquot of same digest was fractionated on SDS-PAGE and stained with Coomassie blue (Figure 1B bottom panel). We next investigated whether this is caused by enzymatic differences (glycosyltransferase and de-glycosylases) between normal and glaucomatous TM tissues.

### 3.2 Enzymatic activities and aberrant glycosylation in the glaucomatous TM

We prepared a curated short list of all glycosyl metabolizing activities known to be present in the human TM at the mRNA level and a comprehensive search was performed for glycosyltransferases in the literature, GEO, and Unigene databases (Supplemental Table S3a). For de-glycosylases, additional searches were performed in BRENDA, Ensembl, and



GEO databases (Supplemental Table S3b). We further verified their local production in the TM using appropriate primer pairs and PCR analysis. We next investigated protein expression for confirmed mRNA presence (data not shown; Table S3a, b) using commercially available antibodies. Measurements of enzymatic activity using available relative non-specific assays showed agreement and correlation with immunoreactivity. The immunoreactivity of glycosyl metabolizing enzymes determined that ELISA analyses correlated with that of the dot blot analyses (Supplemental Figure S1B) and showed differences between glaucomatous and normal TM (Figure 1C, D). We divided these activities in two categories: glycosyltransferases (the enzymes that transfer sugars onto proteins: GLT8D1, GLT8D2, GLT6D1, DDOST and UGT8; Figure 1C; Supplemental Table S3a) and protein de-glycosylases (the enzymes that remove sugars from modified proteins: GLA, NAGA, GLB1, GALNS, FUS2 and FUCA1; Figure 1D; Supplemental Table S3b), respectively. We found a small decrease in glycosyltransferase GLT6D1 and UGT8 levels. UGT8 or UDP-galactose-ceramide galactosyltransferase is known to catalyze the transfer of galactose to ceramide. While this may be relevant for biosynthesis of galactocerebrosides or sphingolipids of myelin membranes, it is irrelevant for the present investigation. GLT6D1 or Galactosyltransferase family 6 domain-containing 1 is the protein product of an uncharacterized gene and has been identified as a susceptibility locus for periodontitis [23]. Significant increased levels of de-glycosylase GLB1 or Beta-galactosidase was found in glaucomatous compared to normal TM (Figure 1D). GLB1 cleaves beta-linked terminal galactosyl residues from glycoproteins, and glycosaminoglycans [24]. Having determined the level of glycosyltransferases and de-glycosylases, our next goal was to determine which proteins are differentially glycosylated between glaucoma and control. However, the determination of differential glycosylation posed another problem, that protein levels themselves could also undergo a differential change between glaucoma and control tissues. We therefore attempted to identify changes in protein levels between glaucomatous and normal TM followed by further analyses of a select subset of proteins for determining their glycosylation states between control and glaucomatous tissue. Quantitative analyses of changes in protein levels enabled us to account for changes in glycosylation of select protein in proportion to their level changes between control and glaucomatous tissue.

### 3.3 Alteration of glycosylation is independent of protein level changes

We next subjected 8-plex iTRAQ labeled quantitative analyses of total TM proteins from glaucomatous (tags 113–116) and normal donors (tags 117–121) to identify the changes in protein levels (Supplemental Table S4) between glaucomatous and control donors. We also attempted 8-plex iTRAQ labeled quantitative proteomic analyses of precipitated lectin-bound proteins from glaucomatous (tags 113–116) and normal TM (tags 117–121) extracts (Supplemental Table S5). The latter attempt was made to capture enriched glycosylated proteins. In both experiments, we identified several known glycosylated proteins and proteoglycans. We compared these quantitative proteins with GEO datasets (GDS359 and GDS 1640). We further compared the results with published reports on TM glycoproteins and proteoglycans [9, 10, 13, 25, 26]. We selected a few protein candidates to determine for their potential hypo-glycosylation in glaucomatous tissue (hyper-glycosylated in normal) in comparison to the controls. The proteins that undergo hyper-glycosylation are also an important component but in the present studies we focused on identification of proteins that

are hypo-glycosylated in glaucomatous TM with the goal of mimicking hypo-glycosylation via inhibitors in primary TM cells to further investigate the effects. We selected Semenogelin 2, Keratocan and Biglycan, which showed less than 2-fold changes in protein levels for further analyses of total glycosylation per protein. Our objective was to find proteins whose level either do not change at all (ratio of 1.0 with iTRAQ labeling) or change less than 2-fold (ratio of 2.0) for investigation of level changes in their glycosylation (Supplemental Table S4). Our bioinformatic analyses (PSORT, String and other databases) revealed that a number of glycoproteins, including Keratocan and Biglycan, have the potential to be secreted into the ECM and have the potential for multiple protein-protein interactions (Supplemental Table S6). We used partial enzymatic PNGase F digestions for removal of N-linked glycosylation following previously published procedures [27], electrophoretic separation, and Western Blot analyses (Figure 2) to determine the protein glycosylation levels. Briefly, the undigested and PNGase F digested collapsed protein bands (Figure 2A, arrows) serve as estimates of total protein and glycosylated fractions of the protein. The ratio of total protein and total protein normalized glycosylated fractions in normal and glaucomatous TM, with or without comparison to total protein load or a house keeping protein (GAPDH or Beta-Actin), provides the relative glycosylation level for the specific protein. The Western Blot analyses of Keratocan without PNGase F (Figure 2A) served as total proteins before digestion. After the PNGase F digestion, the total amount of lower digested band (indicated by arrow head) was estimated using densitometry and used for determination of the ratio of digested band compared to total, providing an estimate of relative protein glycosylation. Keratocan in normal TM tissue was more glycosylated compared to glaucomatous TM (Figure 2A). Biglycan in the TM tissue (Figure 2B), as well as in the primary TM cells with and without inhibitor treatment (Figure 2C), was subjected to similar analyses. A series of partial PNGase F digestion enables confirmation of the estimates. We used microtubule associated protein 2 (MAP2) and Semenogelin II (SEMG2), whose protein levels have been found to not undergo any change (ratio of 1.0 between glaucoma and normal; Supplemental Table S4), as controls and analyzed the ratio of proteins between glaucomatous and normal TM. In all these analyses we have used total protein load as well as GAPDH and Beta-actin as protein loading or normalizing controls. While the MAP2 and SEMG2 were found to be unchanged in Western Blot analyses, the Keratocan and Biglycan protein levels were found to have a ratio of 1.9 and 1.3 respectively between glaucomatous and normal TM (Figure 2D; Supplemental Table S4). Their glycosylation levels, however, clearly demonstrate lower levels in glaucomatous compared to normal TM. We used in vitro experiments for confirmation of detection of glycosylation using partial PNGase F treatment. The Biglycan protein and glycosylation levels were estimated between control untreated and glycosylation inhibitor treated (described in greater detail in the next section) primary TM cells for comparison of protein and glycosylation levels in vitro. The cells showed a higher level of protein in the inhibitor treated cells (ratio of 1.4) while the glycosylation level (Figure 2C) showed a clear decrease in levels in inhibitor treated cells (Figure 2D). Performed simultaneously with analyses for tissues, these results confirm the consistency of the analysis method. Previously optimized [21] staining using Gelcode Glycoprotein and Pro Q Emerald 300 glycoprotein kits estimated Keratocan and Biglycan glycosylation levels to be consistent with Western Blot findings (Figure 2D).

### 3.4 Enzymatic inhibitors mediated global TM glycosylation reduction alters primary TM cell properties and tracer transport across cell layers

We next attempted to determine whether inhibition of glycosylation results in changes in TM cells properties. Primary TM cells were treated with inhibitors of sulfotransferases, glycosyltransferases and sialyltransferases to cause global glycosylation changes. SS, an inhibitor of ST3GAL1, (ST3 beta-galactoside alpha-2.3-sialyltransferase 1) and two synthetic inhibitors, [N-(8-quinolinylsulfonyl)-phenylalanine] (PhQ) and [4-(methylsulfanyl)-2-(quinolin-2-ylformamido)-butanoic acid] (MeQ), for members of GlcNAc-6-O- sulfotransferase family which are specifically known to inhibit *N*-acetylglucosamine-6-O-sulfotransferase-2 (GST-2) and *N*-acetylglucosamine-6-O-sulfotransferase-3 (GST-3), were used for reduction of glycosylation. PNGase F analyses (Figure 2) and further FACE analyses (data not shown) confirmed reduced global TM protein glycosylation as a consequence of treatment of cells with these inhibitors. Treatment of primary TM cells with these inhibitors (concentrations of SS: 150  $\mu$ M, PhQ: 75  $\mu$ M, MeQ: 50  $\mu$ M) showed distinct and significant alteration in the shape of the TM cells, that is, a spindle-like elongation of the cell body (Figure 3A), reduced motility, and increased division time (Figure 3A, Supplemental Videos S1 & S2). These changes were observed at ~4 h after addition of inhibitors in the cell culture. TM cells cultured to a five-layer cell matrix grown on a porous polycarbonate membrane subjected to the three inhibitor treatment showed an increased level of fluorescein transport compared to untreated layer setup (Figure 3B; solid lines). The extended incubation (~ 3 days) of inhibitor treated cells without collagen matrix also showed increased flow of tracer compared to controls as noted for cells without extended incubation (Figure 3B, solid lines). This is consistent with elongated cells rendering larger areas for fluid transport. In a comparison after extended incubation (~3days), an identical setup of TM cells, cultured to a five-layer cell matrix grown on the same porous polycarbonate membrane but coated with cross linked collagen at each layer level, displayed a decreased tracer transport following the combined inhibitor treatment as compared to untreated cells (Figure 3B; dashed lines). This is consistent with compaction of layers and loss of flexibility in cellular modeling upon inhibitor treatment enabling tortuous flow across cell layers thus increasing residence time. Primary TM cells suspended in media-enriched polymerized collagen gel inside glass microcapillaries [28] displayed a lack of gel expansion/contraction in the combined inhibitor treated group and was comparable to untreated cell containing gels, consistent with the lack of flexibility for the inhibitor treated cells. We did not find any significant cell death due to prolonged inhibitor treatment (Figure 3C). There was not a statistically significant difference in cell survival between control and inhibitor treated groups at different time intervals (Figure 3C).

## 4 Discussion

How post-translational modifications, and in particular, global TM glycosylation affect the aqueous outflow dynamics is not fully understood. Alterations in global TM glycosylation levels were found in POAG as well as juvenile glaucoma [29, 30]. Unlike ACG, the iridocorneal angle remains open in the POAG but yet the aqueous outflow is decreased which is thought to be due to increased resistance at the TM. Surface glycoproteins are important determinants of cellular structural and functional properties [15]. Aberrant

functioning of glycan-processing enzymes (glycosidases and glycosyltransferases) involved in the biosynthesis and transfer of the carbohydrate moieties results in aberrant glycosylation [31]. Aberrant glycosylation alters properties of cells such as adhesion, invasion, and capacity to withstand different regimes of fluid shear [7, 32].

Glycocalyx, or the surface protein glycosylation, has been shown to act as a sensor of fluid shear stress in a variety of cells that include endothelial [7], osteoblast [33], and smooth muscle [34] as well as several other cell types [35]. Fluid flow and migration of cells in biological systems is often associated with engagement of specialized adhesion molecules [35]. The floating endothelial cells [7] are known to undergo glycocalyx changes in response to different regimes of changing fluid shear. However, very little is known about the glycocalyx of cells from neural crest origin such as TM cells [36]. The TM cells function in an environment that is continuously subjected to varying levels of fluid shear stress or shear induced mechanical forces [37]. Actin cytoskeletal remodeling and changes in cell shape and mobility occurs in response to mechanotransduction due to a changing regime of fluid shear [7, 8]. Cytoskeletal changes are often commensurate with dynamic changes in surface protein glycosylation [7, 35].

Our understanding of adhesive interactions under different flow conditions is also incomplete and whether glycosylation is an effector of adhesive interactions has not been well studied. Neoplastic transformation is usually associated with altered binding to lectins [38] due to altered surface glycosylation and is also commensurate with altered mobility on soft agar [39]. Metastatic cancer cells undergo migration commensurate with continuous altered expression of adhesion molecules as they undergo different lymphatic fluid shear stress during their migration [40]. Different degrees of L-selectin binding are shown by different cancer cell types when they migrate through different shear threshold regimes. Sialylation, sulfation, and N-glycosylation are effectors of L-selectin binding. Squamous colon and leukemic cancer cells, as well as endothelial cells, show different glycosylation levels of L-selectin as they migrate through different shear thresholds [40].

Our analysis with biotinylated lectins revealed modulation of glycoprotein and proteoglycans in the glaucomatous TM as compared to control specimens (Figure 1A) and is likely to capture the cellular surface glycoprotein changes. The pSORT analyses of proteins identified in our quantitative proteomic analyses suggests cell surface and ECM as well as residence of identified glycoproteins (Supplemental Table S6).

A previous study of lectin-binding on human TM [15] and another on bovine ocular tissues [16] utilized several common lectins used here (Supplemental Table S2). Previous studies [15, 16] utilized DAB methods which are rather subjective compared to clear contrast obtained using fluorescent detection (Figure 1A). We have utilized several previously unavailable lectins [15] and despite their overlapping recognition of the sugar modifications, a number of these lectins present important differences in terms of peptide context for their sugar modification recognition motif. Our overall findings are consistent and in general agreement with previous results (Figure 1A; Supplemental Table S2) that showed elevated glycoproteins in glaucomatous TM. In contrast, our FACE analyses (Figure 1B) supports co-

occurrence of hypo and hyper glycosylation in the glaucomatous TM with respect to several disaccharides.

We further pursued the hypo-glycosylation in glaucomatous TM (Figure 1B) but not hyper-glycosylation (in glaucomatous TM). It would be important and interesting to determine the consequences of observed hyper-glycosylation in glaucomatous TM (Figure 1B) and their reversal as well. However, in the current study we focused on the observed hypo-glycosylation changes observed in glaucomatous TM in contrast to controls. Primary TM cells were subjected to specific glycosylation inhibitors to achieve reduced global TM protein glycosylation (Figure 2D) and to determine consequent changes in the behavior and properties of the TM cells (Figure 3A). These findings are consistent with enzymatic reduction or removal of N-glycosylation affecting cell surface microenvironment, cell adhesion, and cell migration [41]. The fluid transport studies in a multilayer cell arrangement demonstrate modulation of the fluid flow ostensibly due to altered behavior of glycosylation inhibited cells (Figure 3B). Notably, the collagen matrix embedded cells showed decreased tracer transport for inhibitor treated cells compared to controls (Figure 3B; dashed lines). It is possible that used glycosylation inhibitors are toxic to the cells. However, we did not see any discernable cell death of primary TM cells with the concentration ranges used. We have also used primary retinal pigment epithelium (RPE) as well HEK293 cells as controls. RPE or HEK293 cells did not show changes in cell shape or behavior similar to that demonstrated by TM cells nor did layered RPE primary cells demonstrate any changes in tracer transport under identical setting (data not shown).

Fluid shear is a form of mechanical stimulus, however, mechanical stimuli in the form of biophysical cues also have been suggested to play a role in the TM cell expansion and remodeling [37]. The trabecular cell surfaces as well as the inter-trabecular spaces are lined with mucinous GAGs (glycosaminoglycans) [42, 43]. Whether GAGs are associated with biophysical cues remain to be determined. Biophysical cues have been shown to result in changes in shape and motility of TM cells [37]. Notably, laser trabeculoplasty (LT) is one of the effective intervention strategies in glaucoma. Low threshold laser trabeculoplasty has been proposed to provide some sort of local mechanical stimulus to TM cells without causing damage or burn to them. Specific changes due to LT have not been clearly discernable at an ultrastructural level [44], but global TM glycosylation changes have been confirmed and detected both at cellular [45] and at tissue level in cat eyes [21] subjected to LT. The LT associated glycosylation changes remain to be revisited using different interdisciplinary approaches. Changes have been found in cell shape and behavior after LT treatment [45, 46]. It is important to note that absence of ophthalmic and other history of donor eyes remains a problem for overall interpretation and analyses. Usually donor eyes arrive and information follows. Of the 32 total glaucoma eyes procured for these studies we could get the static perimetry results confirming glaucomatous optic neuropathy (mean defect in Supplemental Table S1) and other pertinent ophthalmic information for only about 20 of them (62.5%). Two glaucoma eyes subjected to LT were excluded from final analyses therefore we could use only 56.3% of the procured glaucomatous donor eyes for our final analyses. Another problem with glaucomatous eyes is the frequent incomplete information about treatment medications, which poses some problems in stratifying results. With

recognition of these challenges, we have now initiated efforts in procuring glaucomatous donor eyes with more complete information and also for a greater medical history period.

In summary, the results presented here suggest that altered glycosylation is associated with gross changes in the TM cell shape, motility, and their interaction with matrix contributing to the opening and closing of spaces between cells and thus the general filter behavior of the TM in glaucoma. Modulation in transport of sodium fluorescein across a layer of TM cells embedded in collagen matrix suggests glycosylation to play a role in control of fluid flow across TM tissue. The non-glaucomatous DBA/2-Gpnmb<sup>+</sup>-Sj/J mouse will be a good model system to study the glycosylation inhibitors studies for determination of their effect on the aqueous outflow pathway. Any affect in a model animal system will suggest an underlying dynamic glycosylation sensitive mechanism in the regulation of the aqueous outflow.

## Supplementary Material

Refer to Web version on PubMed Central for supplementary material.

## Acknowledgments

We thank Manik Goel, Gabriel Gaidosh, Avinash Saraon, Qin Yang, Praseeda Venugopalan, Hayden Sandler, Alejandro Lamas, and Julee Sunny for their assistance with experiments and William Feuer for assistance with statistical analyses. This study was supported by NIH grants EY016112, EY016112S1, P30-EY14801 and a career award and unrestricted funds from Research to Prevent Blindness.

## Abbreviations

<b>TM</b>	Trabecular Meshwork
<b>IOP</b>	Intraocular Pressure
<b>PTMs</b>	Post Translational Modifications
<b>ECM</b>	Extracellular Matrix
<b>POAG</b>	Primary open angle glaucoma
<b>ACG</b>	Angle closure glaucoma
<b>NDRI</b>	National Disease and Research Interchange
<b>DAB</b>	3,3'-Diaminobenzidine
<b>HRP</b>	Horseradish Peroxidase
<b>FACE</b>	Fluorophore Assisted Carbohydrate Electrophoresis
<b>GEO</b>	Gene Expression Omnibus
<b>PBS</b>	Phosphate Buffered Saline
<b>BSA</b>	Bovine Serum Albumin
<b>SS</b>	Soyasopinin I
<b>ST3GAL1</b>	ST3 beta-galactoside-alpha-2,3-sialyltransferase 1

<b>PhQ</b>	N-(8-quinolinylsulfonyl)-phenylalanine
<b>MeQ</b>	4-(methylsulfanyl)-2-(quinolin-2-ylformamido)-butanoic acid
<b>GST-2</b>	N-acetylglucosamine-6-O-sulfotransferase-2
<b>GST-3</b>	N-acetylglucosamine-6-O-sulfotransferase-3
<b>LT</b>	Laser Trabeculoplasty
<b>MAP2</b>	microtubule associated protein 2
<b>SEMG2</b>	Semenogelin II
<b>GAGs</b>	Glycosaminoglycans

## References

1. Stadtman ER. Protein modification in aging. *J Gerontol.* 1988; 43:B112–B20. [PubMed: 3047204]
2. Bhattacharya SK. Retinal deimination in aging and disease. *IUBMB Life.* 2009; 61:504–9. [PubMed: 19391158]
3. Jaisson S, Gillery P. Evaluation of nonenzymatic posttranslational modification-derived products as biomarkers of molecular aging of proteins. *Clin Chem.* 2010; 56:1401–12. [PubMed: 20562349]
4. Quigley HA, Broman AT. The number of people with glaucoma worldwide in 2010 and 2020. *Br J Ophthalmol.* 2006; 90:262–7. [PubMed: 16488940]
5. Morrison JC, Johnson EC, Cepurna W, Jia L. Understanding mechanisms of pressure-induced optic nerve damage. *Prog Retin Eye Res.* 2005; 24:217–40. [PubMed: 15610974]
6. Goel M, Picciani RG, Lee RK, Bhattacharya SK. Aqueous humor dynamics: a review. *Open Ophthalmol J.* 2010; 4:52–9. [PubMed: 21293732]
7. Tarbell JM, Weinbaum S, Kamm RD. Cellular fluid mechanics and mechanotransduction. *Ann Biomed Eng.* 2005; 33:1719–23. [PubMed: 16389519]
8. Yao Y, Rabodzey A, Dewey CF Jr. Glycocalyx modulates the motility and proliferativeresponse of vascular endothelium to fluid shear stress. *Am J Physiol Heart Circ Physiol.* 2007; 293:H1023–H30. [PubMed: 17468337]
9. Diskin S, Kumar J, Cao Z, Schuman JS, Gilmartin T, Head SR, et al. Detection of differentially expressed glycogenes in trabecular meshwork of eyes with primary open-angle glaucoma. *Invest Ophthalmol Vis Sci.* 2006; 47:1491–9. [PubMed: 16565384]
10. Acott TS, Kelley MJ. Extracellular matrix in the trabecular meshwork. *Exp Eye Res.* 2008; 86:543–61. [PubMed: 18313051]
11. Haddadin RI, Oh DJ, Kang MH, Filippopoulos T, Gupta M, Hart L, et al. SPARC-null mice exhibit lower intraocular pressures. *Invest Ophthalmol Vis Sci.* 2009; 50:3771–7. [PubMed: 19168904]
12. Wirtz MK, Bradley JM, Xu H, Domreis J, Nobis CA, Truesdale AT, et al. Proteoglycan expression by human trabecular meshworks. *Curr Eye Res.* 1997; 16:412–21. [PubMed: 9154378]
13. Bhattacharya SK, Rockwood EJ, Smith SD, Bonilha VL, Crabb JS, Kuchtey RW, et al. Proteomics reveals cochlin deposits associated with glaucomatous trabecular meshwork. *J Biol Chem.* 2005; 280:6080–4. [PubMed: 15579465]
14. Gygi SP, Rochon Y, Franza BR, Aebersold R. Correlation between protein and mRNA abundance in yeast. *Mol Cell Biol.* 1999; 19:1720–30. [PubMed: 10022859]
15. Chapman SA, Bonshek RE, Stoddart RW, O'Donoghue E, Goodall K, McLeod D. Glycans of the trabecular meshwork in primary open angle glaucoma. *Br J Ophthalmol.* 1996; 80:435–44. [PubMed: 8695566]
16. Tuori A, Virtanen I, Uusitalo H. Lectin binding in the anterior segment of the bovine eye. *Histochem J.* 1994; 26:787–98. [PubMed: 7883589]

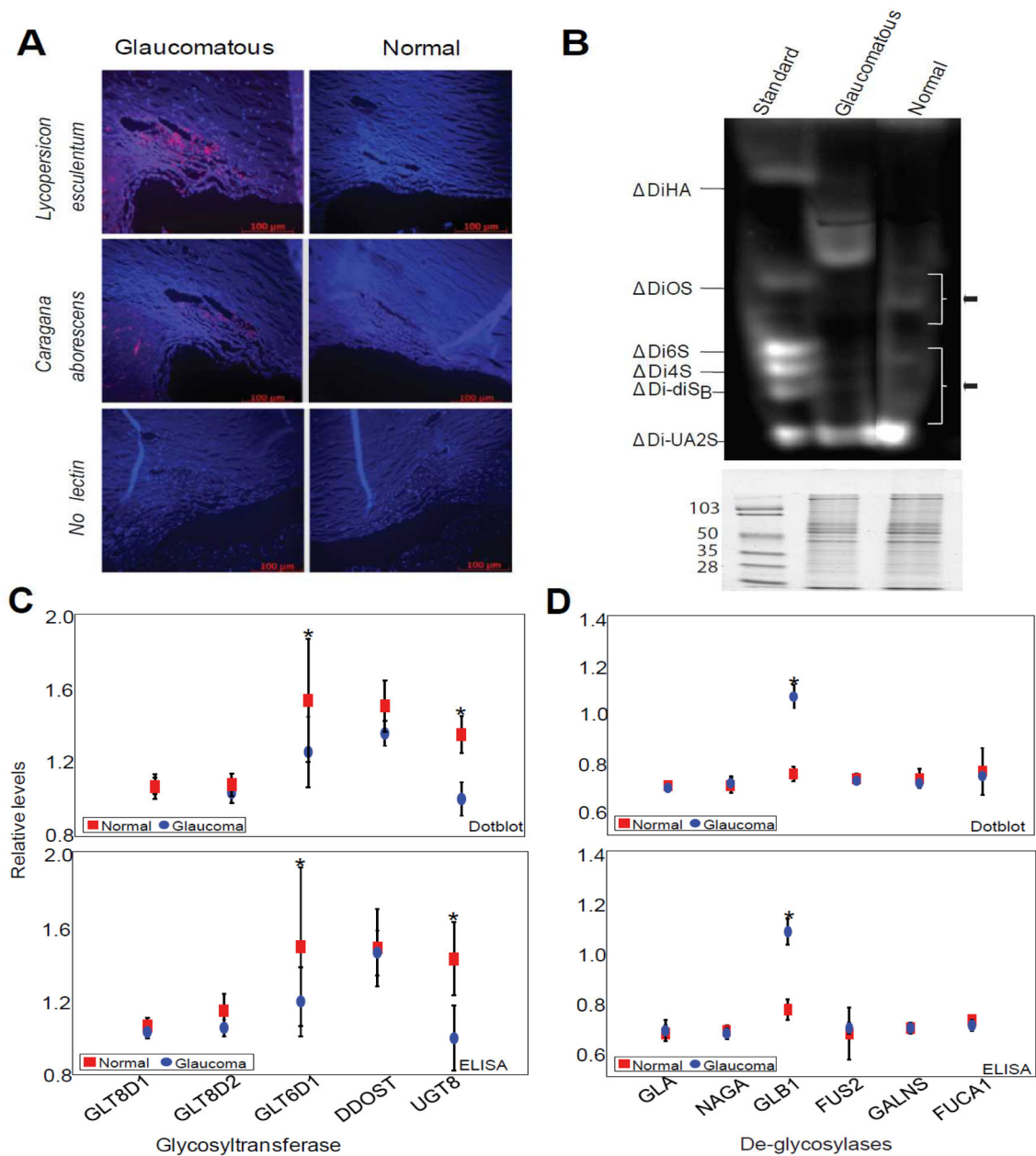
17. Calabro A, Benavides M, Tammi M, Hascall VC, Midura RJ. Microanalysis of enzyme digests of hyaluronan and chondroitin/dermatan sulfate by fluorophore-assisted carbohydrate electrophoresis (FACE). *Glycobiology*. 2000; 10:273–81. [PubMed: 10704526]
18. Calabro A, Hascall VC, Midura RJ. Adaptation of FACE methodology for microanalysis of total hyaluronan and chondroitin sulfate composition from cartilage. *Glycobiology*. 2000; 10:283–93. [PubMed: 10704527]
19. Parikh T, Eisner N, Venugopalan P, Yang Q, Lam BL, Bhattacharya SK. Proteomic analyses of corneal tissue subjected to alkali exposure. *Invest Ophthalmol Vis Sci*. 2010; 52:1819–31. [PubMed: 20861482]
20. Tang WH, Shilov IV, Seymour SL. Nonlinear fitting method for determining local false discovery rates from decoy database searches. *J Proteome Res*. 2008; 7:3661–7. [PubMed: 18700793]
21. Amelinckx A, Castello M, Arrieta-Quintero E, Lee T, Salas N, Hernandez E, et al. Laser trabeculoplasty induces changes in the trabecular meshwork glycoproteome: a pilot study. *J Proteome Res*. 2009; 8:3727–36. [PubMed: 19432485]
22. Aljohani AJ, Munguba GC, Guerra Y, Lee RK, Bhattacharya SK. Sphingolipids and Ceramides of Human Aqueous Humor. *Mol Vis*. 2013; 19:1966–84. [PubMed: 24068864]
23. Schaefer AS, Richter GM, Nothnagel M, Manke T, Dommisch H, Jacobs G, et al. A genome-wide association study identifies GLT6D1 as a susceptibility locus for periodontitis. *Hum Mol Genet*. 2010; 19:553–62. [PubMed: 19897590]
24. Hinek A. Biological roles of the non-integrin elastin/laminin receptor. *Biol Chem*. 1996; 377:471–80. [PubMed: 8922281]
25. Keller KE, Aga M, Bradley JM, Kelley MJ, Acott TS. Extracellular matrix turnover and outflow resistance. *Exp Eye Res*. 2009; 88:676–82. [PubMed: 19087875]
26. Rhee DJ, Haddadin RI, Kang MH, Oh DJ. Matricellular proteins in the trabecular meshwork. *Exp Eye Res*. 2009; 88:694–703. [PubMed: 19101543]
27. Alcazar O, Hawkrigde AM, Collier TS, Cousins SW, Bhattacharya SK, Muddiman DC, et al. Proteomics characterization of cell membrane blebs in human retinal pigment epithelium cells. *Mol Cell Proteomics*. 2009; 8:2201–11. [PubMed: 19567368]
28. Ilagan R, Guthrie K, Quinlan S, Rapoport HS, Jones S, Church A, et al. Linear measurement of cell contraction in a capillary collagen gel system. *Biotechniques*. 2010; 48:153–5. [PubMed: 20359300]
29. Kuleshova ON, Zaidman AM, Korel AV. Glycosaminoglycans of the trabecular meshwork of the eye in primary juvenile glaucoma. *Bull Exp Biol Med*. 2007; 143:381–4. [PubMed: 18225769]
30. Kuleshova ON, Nepomnyashchikh GI, Aidagulova SV. Ultrastructure of connective tissue of eye drainage system in ophthalmic hypertension associated with primary juvenile glaucoma. *Bull Exp Biol Med*. 2008; 145:374–6. [PubMed: 19039948]
31. Spicer SS, Schulte BA. Diversity of cell glycoconjugates shown histochemically: a perspective. *J Histochem Cytochem*. 1992; 40:1–38. [PubMed: 1370305]
32. Hsu CC, Lin TW, Chang WW, Wu CY, Lo WH, Wang PH, et al. Soyasaponin-I-modified invasive behavior of cancer by changing cell surface sialic acids. *Gynecol Oncol*. 2005; 96:415–22. [PubMed: 15661230]
33. Wang H, Young SR, Gerard-O’Riley R, Hum JM, Yang Z, Bidwell JP, et al. Blockade of TNFR1 signaling: A role of oscillatory fluid shear stress in osteoblasts. *J Cell Physiol*. 2011; 226:1044–51. [PubMed: 20857415]
34. Shi ZD, Abraham G, Tarbell JM. Shear stress modulation of smooth muscle cell marker genes in 2-D and 3-D depends on mechanotransduction by heparan sulfate proteoglycans and ERK1/2. *PLoS One*. 2010; 5:e12196. [PubMed: 20808940]
35. Toh YC, Voldman J. Fluid shear stress primes mouse embryonic stem cells for differentiation in a self-renewing environment via heparan sulfate proteoglycans transduction. *Faseb J*. 2011; 25:1208–17. [PubMed: 21183594]
36. Tripathi BJ, Tripathi RC. Neural crest origin of human trabecular meshwork and its implications for the pathogenesis of glaucoma. *Am J Ophthalmol*. 1989; 107:583–90. [PubMed: 2729407]
37. Gasiorowski JZ, Russell P. Biological properties of trabecular meshwork cells. *Exp Eye Res*. 2009; 88:671–5. [PubMed: 18789927]



38. Rambaruth ND, Dwek MV. Cell surface glycan-lectin interactions in tumor metastasis. *Acta Histochem.* 2011 In press.
39. Agre P, Williams TE. The human tumor cloning assay in cancer drug development. A review. *Invest New Drugs.* 1983; 1:33–45. [PubMed: 6381376]
40. Resto VA, Burdick MM, Dugia NM, McCammon SD, Fennewald SM, Sackstein R. L-selectin-mediated lymphocyte-cancer cell interactions under low fluid shear conditions. *J Biol Chem.* 2008; 283:15816–24. [PubMed: 18385135]
41. Krahling H, Mally S, Eble JA, Noel J, Schwab A, Stock C. The glycocalyx maintains a cell surface pH nanoenvironment crucial for integrin-mediated migration of human melanoma cells. *Pflugers Arch.* 2009; 458:1069–83. [PubMed: 19562366]
42. Zimmerman CC, Lingappa VR, Richards JE, Rozsa FW, Lichter PR, Polansky JR. A trabecular meshwork glucocorticoid response (TIGR) gene mutation affects translocational processing. *Mol Vis.* 1999; 5:19. [PubMed: 10459044]
43. Knepper PA, Goossens W, Hvizd M, Palmberg PF. Glycosaminoglycans of the human trabecular meshwork in primary open-angle glaucoma. *Invest Ophthalmol Vis Sci.* 1996; 37:1360–7. [PubMed: 8641839]
44. Stoiber J, Fernandez V, Lamar PD, Decker SJ, Dubovy S, Hitzl W, et al. Trabecular meshwork alteration and intraocular pressure change following pulsed near-infrared laser trabeculoplasty in cats. *Ophthalmic Surg Lasers Imaging.* 2005; 36:471–81. [PubMed: 16358427]
45. Van Buskirk EM, Pond V, Rosenquist RC, Acott TS. Argon laser trabeculoplasty. Studies of mechanism of action. *Ophthalmology.* 1984; 91:1005–10. [PubMed: 6493712]
46. Acott TS, Samples JR, Bradley JM, Bacon DR, Bylsma SS, Van Buskirk EM. Trabecular repopulation by anterior trabecular meshwork cells after laser trabeculoplasty. *Am J Ophthalmol.* 1989; 107:1–6. [PubMed: 2912110]

### Clinical Relevance

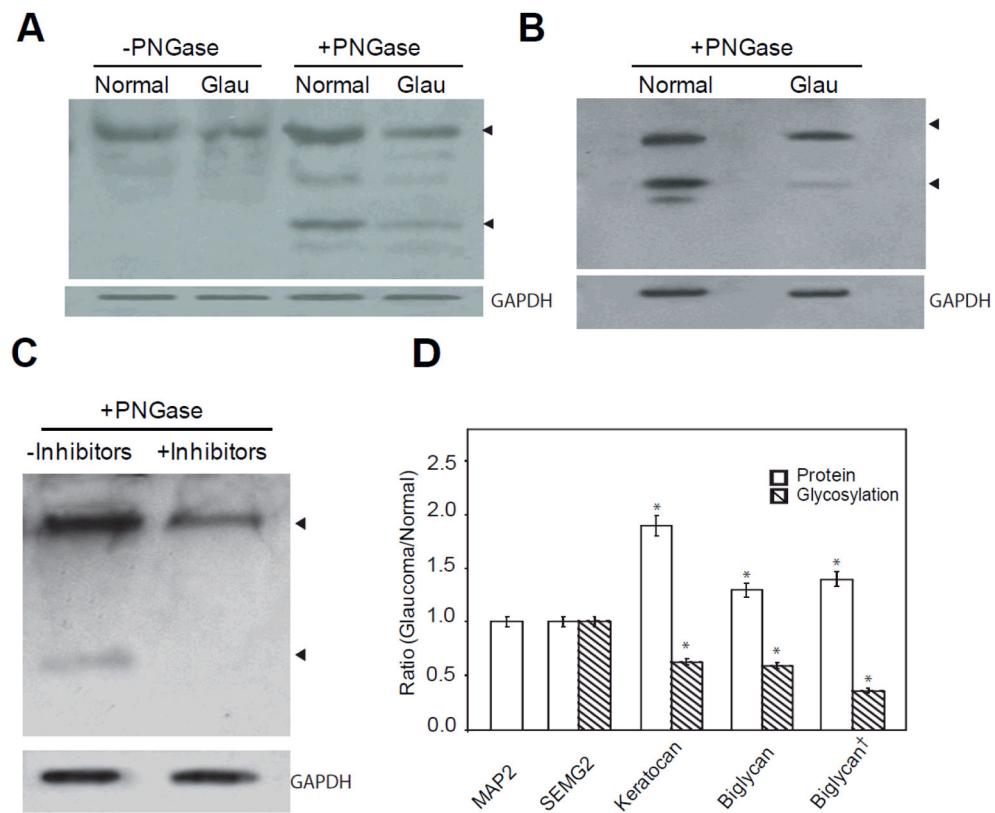
Unlike high throughput mRNA and protein analyses, those of posttranslational modifications (PTMs), objective of current work, are relatively scant. Often it is the posttranslationally modified protein that is active (or inactive) compared to the non-modified version of the protein. Understanding the PTM differences between normal and glaucomatous trabecular meshwork tissue will give mechanistic insight into the pathology of glaucoma. Understanding the glycosylated state of proteins will also enable finding innovative ways to restore the normal glycosylation condition and determine whether reinstating the normal state may help restore conditions associated with pathology.



**Figure 1.**

Glycosylation levels and protein glycosylation enzymatic activities in control and glaucomatous trabecular meshwork (TM). (A) Representative microscopic image of histochemical analyses (n=12 each glaucoma and control) of bound fluorescent-lectins in the TM. The cadaver TM from glaucomatous or control donors as indicated was probed using biotinylated lectins as indicated. The detection was based on Alexa<sup>®</sup>-594 coupled streptavidin binding to biotinylated lectin. Images were taken on Leica TSP5 confocal microscope (Leica Corporation, Manheim, Germany) at 20x magnification. A tissue section that was not probed with any lectin served as negative control. (B) Representative Fluorophore-assisted carbohydrate electrophoresis (FACE<sup>®</sup>) analyses of 2-aminoacridone

(AMAC) derivatized testicular hyaluronidase and chondroitinase ABC digested products from normal and glaucomatous TM as indicated. The disaccharide standards were obtained from Hyal-Dermato Disaccharide D-kit (cat# 400572-1; Seikagaku Corporation) To indicate equal loading, an identical aliquot was loaded on to a 10% SDS-PAGE and stained with Coomassie blue for protein staining with molecular markers as indicated presented in the bottom panel. **(C)** Relative quantification of glycosyltransferase immunoreactivities using ELISA and dotblot densitometric analyses as indicated. **(D)** Relative quantification of deglycosylase immunoreactivities using ELISA and dot blot densitometric analyses as indicated. The enzymatic immunoreactivity ratio (normalized to total protein/total of GAPDH) of indicated enzymes (C, D) with GAPDH was quantified using ELISA and dot blot analysis as indicated and as described in experimental procedures (n= 12 samples each for glaucoma and control). Results are mean  $\pm$  standard deviation (\*Significantly different results when compared between control and glaucoma donors by the two-tailed two sample t-test: \*p<0.05). Control and glaucomatous samples are represented by red squares and blue circles for dot blots and ELISA analyses as indicated.

**Figure 2.**

Glycosylation differences of select target proteins in glaucomatous TM compared to controls (n= 12 each) and in response to glycosylation inhibitors. **(A)** Representative Western analyses of Keratocan in control and glaucomatous TM protein extracts (10 $\mu$ g) with or without PNGase F treatment as indicated. The ratio of intact to collapsed protein band on digestion provided the ratio of glycosylation for normal or glaucoma. The ratio of intact band between glaucoma to normal provided the level of protein (normalized to total protein, GAPDH or Beta-actin). **(B)** Representative Western analyses of Biglycan in control and glaucomatous TM protein extracts with PNGase F treatment. **(C)** Representative Western analyses of Biglycan in control and inhibitor treated (SS: 150 $\mu$ M, PhQ: 75  $\mu$ M, MeQ: 50  $\mu$ M) cell extracts subjected to PNGase F treatment. Glycerol 3-phosphate dehydrogenase (GAPDH) immunoreactivity as indicator of loading control for panels A through C have been presented as indicated. **(D)** Densitometric estimation of proteins (hollow bars) and glycosylation (hashed bars) expressed as ratio for each specific protein as indicated. The ratios for proteins and glycosylation are immunoreactivity in glaucoma/normal, except for Biglycan $\dagger$ , which indicates ratio of inhibitor treated/untreated control. The glycosylation level in normal or glaucoma was the normalized ratio of glycosylation estimated by partial digestion of PNGase treatment compared to undigested control band (as shown for Keratocan in A). The overall ratio of glycosylation estimated in glaucoma to control (for Biglycan $\dagger$ , inhibitor treated to control) using this procedure has been depicted with hashed bars. The results are mean $\pm$  SD of three independent experiments. The mean ratio was subjected to a two-tailed paired t-test; \*P < 0.05.

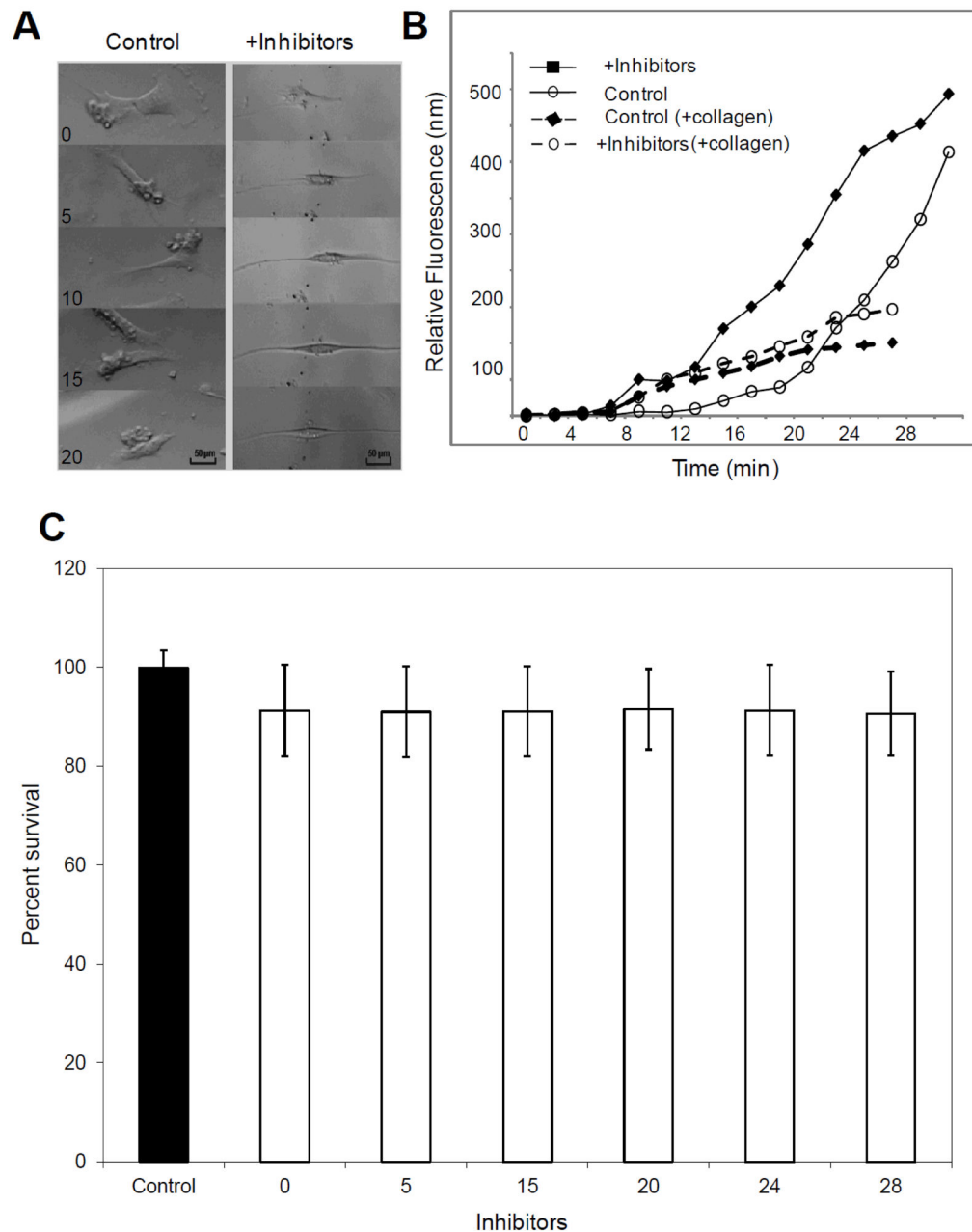


**Figure 3.** Effects of inhibitor mediated reduction in glycosylation in vitro (representative data). **(A)** Representative microscopic images depicting cell morphology in response to inhibitor mediated reduction in protein glycosylation in comparison to controls as indicated in selected hourly time intervals **(B)** The transport of fluorophore across multilayered ensemble of primary TM cells with or without glycosylation inhibitor treatment on a porous 8  $\mu$ m membrane, without any collagen embedding (solid lines) and with collagen matrix embedding at each cell layer (dashed lines). **(C)** The cell survival for primary TM cells were determined for control (filled bars) and inhibitor treated groups at indicated time interval

(hollow bars) in hours using Trypan blue exclusion assay. The average $\pm$  standard deviation of percent of cell survival for indicated groups have been shown.